

# Accurate prediction of multicaloric response and thermodynamics in FeRh

Nikolai A. Zarkevich<sup>1,\*</sup> and Duane D. Johnson<sup>1,2,†</sup>

<sup>1</sup>Ames Laboratory, U.S. Department of Energy, Iowa State University, Ames, Iowa 50011-3020, USA

<sup>2</sup>Materials Science and Engineering, Iowa State University, Ames, Iowa 50011-2300, USA

(Dated: May 14, 2022)

Stoichiometric B2 FeRh is simple structurally but exhibits a metamagnetic transition at 353 K from antiferromagnet (AFM) with (111) spin ordering to a ferromagnet (FM), yielding multicaloric, i.e., magneto-, elasto-, and baro-caloric, responses. At cryogenic temperatures and ambient pressure, it is also unstable to several competing AFM orthorhombic and tetragonal structures, from an inherent M-point phonon instability. With its chemical simplicity and multi-state competition, FeRh serves as a wonderful “fruit fly” in the materials genome discovery of caloric systems, on which we test our ability to assess the metamagnetic transformation and associated caloric properties. Applying estimators for thermodynamic quantities, we predict the metamagnetic transition at 346 K and caloric properties, including the isothermal entropy change and isentropic temperature change, which are in quantitative agreement with experiment.

Keywords: FeRh, ground state, caloric, metamagnetic, phase transformation

## I. INTRODUCTION

Intriguingly, FeRh and NiTi austenite have the same nominal chemical B2 structure (CsCl,  $Pm\bar{3}m$  space group, see Fig. 1) and exhibit a large caloric effect<sup>1–8</sup>. While both show elasto- and baro-caloric response, antiferromagnetic (AFM) FeRh exhibits a strong magnetocaloric effect at its metamagnetic transition to a ferromagnetic (FM) state at the critical temperature  $T_c$  of 353 K, with a 1% decrease in density<sup>2</sup>. Moreover, B2-austenite FeRh (below 353 K) and NiTi (above 313 K) both have unstable phonon modes. In NiTi, the austenite-to-martensite transformation path, resulting in its shape-memory and elastocaloric behavior, has a sensitivity to atomic displacements  $d$ <sup>9,10</sup>. Surprisingly, the NiTi austenitic structure (nominally with B2 chemical order) has large, athermal, short-ranged correlated atomic  $d$ 's; and such a structure provided quantitative agreement to thermodynamic measurements and diffraction data<sup>10</sup>. AFM-B2 FeRh reveals a similar premartensitic instability, a surprise after all the years of experimental<sup>1–5,11–27</sup> and theoretical<sup>6,28–41</sup> studies.

The metamagnetic  $T_c$  of FeRh is sensitive to stoichiometry, lowering precipitously with small additions of at.% Rh<sup>15</sup>. Due to a large entropy change  $\Delta S_T$  (and associated isentropic  $\Delta T_S$ ) at this transition, a large caloric temperature drop (12.9 K at 1.95 Tesla) is found in quenched Fe<sub>49</sub>Rh<sub>51</sub><sup>3</sup>. While bulk FeRh is prohibitively expensive (Rh price is \$30/g in 2017<sup>42</sup>, after peaking at \$350/g in 2008<sup>43</sup>), Fe–Rh may find use in caloric thin-film<sup>3,5,20,44–47</sup> and nanoscale devices<sup>27,40,48–55</sup>. Nonetheless, with its chemical simplicity and multi-state competition, FeRh serves as a wonderful “fruit fly” in the materials genome discovery of better caloric systems, especially to identify the origins for unique behavior and key competing structures.

We recently found<sup>56</sup> that B2 FeRh with AFM(111) spin order has a premartensitic instability at ambient pressure below 90 K to an orthorhombic ( $Pm\bar{m}n$ ) struc-

ture, in line with recent reports of unstable M-point phonons<sup>39–41</sup>. We identified the stable structure and barrierless minimum-enthalpy path<sup>56</sup> of the martensitic transformation, using simulated annealing via *ab initio* molecular dynamics and solid-state nudged-elastic band methods<sup>57,58</sup>. We confirmed that several structures are closely competing, including a proposed AFM(100) highly distorted ( $c/a = 1.23$ ) body-centered tetragonal (BCT) structure<sup>41</sup>. Our results<sup>56</sup> establish that the BCT structure is not a groundstate, but a higher-energy constrained solution.

With relevant competing structures and magnetic states identified, the more symmetric cubic B2 has lower Gibbs free energy at room temperature due to larger phonon entropy (see below), in agreement with the observed austenitic AFM(111) B2 phase<sup>15,21,59</sup>.

Here we focus on estimators to predict thermodynamic quantities. We find that quantities relevant to the caloric response associated with the metamagnetic transition can be calculated in a quantitative agreement with measurements (Table I). We also provide insight into the key requirements needed to predict caloric behavior accurately. Such information helps to identify computationally fast screening measures and correlations that assist in materials discovery<sup>60</sup> via machine learning.

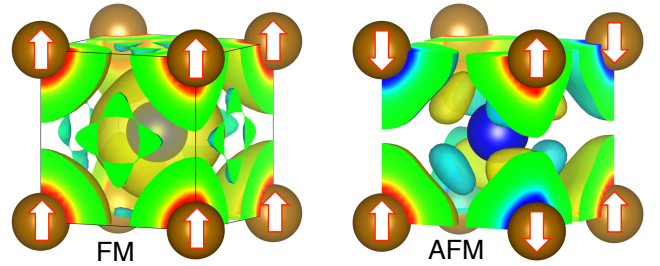


FIG. 1. (Color online).  $\pm 0.002e^-/\text{\AA}$  isosurfaces of electronic spin density in FM (left) and AFM (right) B2 FeRh.

## II. RESULTS

Among thermodynamic quantities calculated, we will address the maximal isentropic temperature change  $\Delta T_S = -T_c \Delta S_T / C_B$  of  $-13$  K, which compares well to experiment<sup>3,5,46</sup>. Here  $T_c$  is the phase transition temperature, which we estimate at 346 K compared to 353 K in experiment<sup>15</sup>;  $C_B$  is the heat capacity at magnetic field  $B$ , and  $\Delta S_T = \Delta S_L + \Delta S_e + \Delta S_m = 0.227 k_B/\text{FeRh}$  is the total isothermal entropy change at  $T_c$  from lattice (L), electronic ( $e$ ) and magnetic ( $m$ ) contributions. We find that  $\Delta S_e$  of  $0.163 k_B/\text{FeRh}$  is the largest, and  $\Delta S_m$  is the smallest (for the FM-AFM metamagnetic transformation). And, the lattice  $\Delta S_L = 0.064 k_B/\text{FeRh}$  is the most tricky to evaluate. Thus, we first address phonons, and some of the important issues to the calculated  $\Delta S_L$ , especially regarding its sensitivity to atomic displacements  $d$ . Next, we calculate thermal expansion, magnetostructural transformation and its  $T_c$ ,  $dT_c/dB$ , entropy changes and related caloric properties.

### A. Phonons

Vibrational entropy in materials can contribute significantly to their caloric response. As shown below, AFM-B2 austenite is stabilized by entropy at room temperature, overcoming an inherent M-point phonon instability at low temperatures. As such, AFM(111) B2 FeRh must have a premartensitic instability, similar to that in NiTi austenite<sup>9,10</sup>, but smaller (see Fig. 2a in<sup>10</sup>). Hence, care must be taken to calculate accurately the lattice contributions to thermodynamic quantities. Simply calculating phonons at a given lattice constant ‘ $a$ ’ and temperature ‘ $T$ ’ is insufficient.

Distinct from previous work, we evaluate phonons and their sensitivity to the  $d$  used to calculate them. Using the *small*-displacement method<sup>61</sup> at pressure  $P=0$ , we find an unstable phonon mode at  $M$  ( $\frac{1}{2}\frac{1}{2}0$ ) in the AFM phase (Fig. 2), but not in the FM phase (Fig. 3), similar to recent results<sup>39-41</sup>. (The predicted AFM(111) orthorhombic groundstate is stable<sup>56</sup>.) At ambient conditions, the FM FeRh phase is stable, but not harmonic, with instabilities nearby (e.g., due to strain<sup>39</sup>). For the least harmonic phonons, frequency dependence on  $d$  is the strongest. The high-frequency optical phonon modes are harmonic in both FM and AFM phases, while the low-frequency acoustic phonons show less harmonic behavior around  $M$ , where the difference between modes, calculated for  $d = 0.04$  and  $0.12$  Å, is the largest (Fig. 2).

To calculate phonons, one could use results from an *ab initio* molecular dynamics at a given  $T$  in the ThermoPhonon code<sup>10,62</sup>. A faster but more approximate method, which we use at  $T_c$  of 353 K, is an application of the quasiharmonic approximation to single-atom displacements  $d$  with a “thermal” potential energy  $E(d) = \frac{1}{2}k_B T$  in an ideal structure (see Fig. 4). This method is applied to FeRh in Fig. 3 and shows that AFM B2

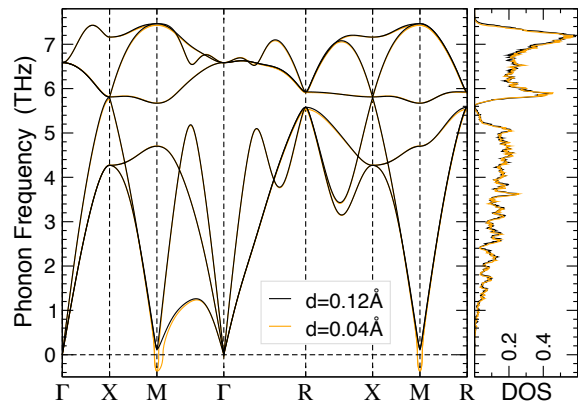


FIG. 2. (Color online). Phonon frequencies and DOS for AFM B2 FeRh, calculated at  $a = 2.996$  Å ( $P=0$ ) using small ( $0.04$ Å) and large ( $0.12$ Å) atomic displacements. Unstable phonons at  $M$  ( $\frac{1}{2}\frac{1}{2}0$ ) appear at  $d \leq 0.06$  Å.

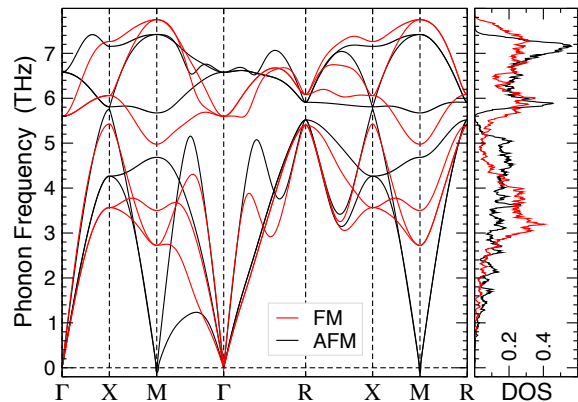


FIG. 3. (Color online). B2-FeRh phonon frequencies and DOS for FM and AFM states at  $a = 2.997$  Å, for  $d(\text{Fe}) \approx d(\text{Rh}) \approx 0.06$  Å at  $\frac{1}{2}k_B T_c$ , see Fig. 4.

structure has an unstable phonon mode at  $M$  with an amplitude of only  $0.1 i$  THz (i.e., close to zero) at “thermal” displacements  $d(T_c) \approx 0.06$  Å [here  $d(\text{Fe}) \neq d(\text{Rh})$ , see Fig. 4]; this instability becomes larger at smaller  $d$  (including infinitesimal) and disappears at larger  $d$ .

Recall that soft phonon modes affect the lattice entropy  $S_L$ . The *large*-displacement method within the quasiharmonic approximation is a computational trick to avoid the unstable phonons. The displacement  $d$  can be adjusted to temperature  $T$  (Fig. 4) in an effort to evaluate the lattice entropy  $S_L(T)$ , see Fig. 5. This  $T$ -dependent entropy is calculated at fixed lattice constants (neglecting the thermal expansion).

Next, we use the phonon DOS (Fig. 3) to evaluate a change in the lattice entropy  $\Delta S_L$  at the metamagnetic transition at  $T_c$  (Fig. 6). The calculated lattice entropy  $S_L$  of the anharmonic FM phase depends on the choice of  $d$  (see Fig. 5), changing from  $8.859 k_B/\text{FeRh}$  for small  $d = 0.04$  Å to  $8.972 k_B/\text{FeRh}$  for large  $d = 0.12$  Å at fixed  $a = 2.997$  Å. For AFM, we find a small change

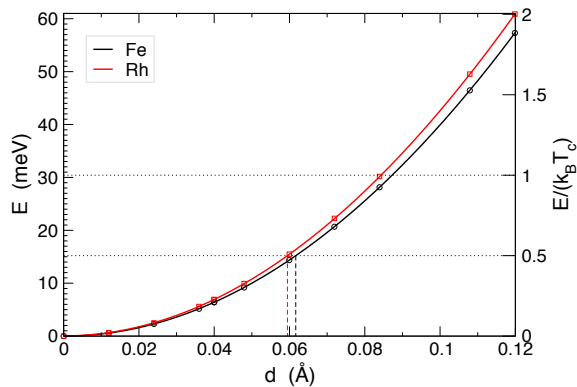


FIG. 4. (Color online). Energy of displacement  $d$  of a single Fe (black) or Rh atom (red line) along [100] in FM B2 structure at  $a = 2.997 \text{ \AA}$ , compared to  $k_B T_c$ .

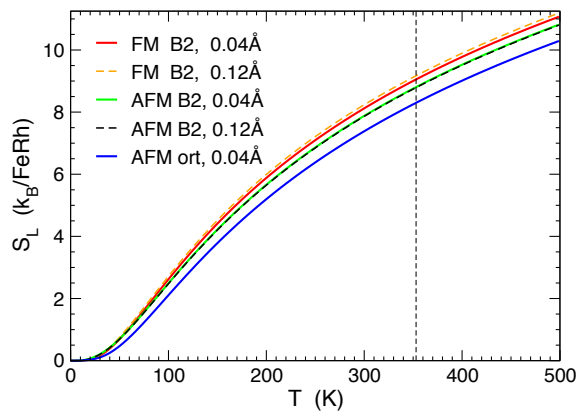


FIG. 5. (Color online). Lattice entropy  $S_L$  of the fully relaxed FM B2, AFM B2, and AFM orthorhombic structures at  $P=0$ , calculated using small ( $0.04 \text{ \AA}$ ) and large ( $0.12 \text{ \AA}$ )  $d$ 's.

from  $8.8176$  to  $8.7945 k_B/\text{FeRh}$  for those fixed  $d$ . Values from the small- $d$  ( $0.04 \text{ \AA}$ ) method give a smaller  $\Delta S_L$  of  $0.042 k_B/\text{FeRh}$  (or  $0.02 k_B$  per atom). However, with  $T$ -dependent displacements  $d(T_c) \approx 0.06 \text{ \AA}$ ,  $\Delta S_L(T_c)$  increases to  $0.064 k_B/\text{FeRh}$  ( $0.03 k_B$  per atom), see Fig. 6.

## B. Thermal expansion

From our calculated energy ( $E$ ) versus volume ( $V$ ) curves in Fig. 7, the equilibrium lattice constants  $a_0$  at zero pressure are calculated as  $2.996 \text{ \AA}$  and  $3.012 \text{ \AA}$  in the AFM and FM B2 phases, respectively, while the measurements on  $\text{Fe}_{50}\text{Rh}_{50}$  at  $353 \text{ K}$  give  $2.987 \text{ \AA}$  and  $2.997 \text{ \AA}$  (similar to earlier values<sup>16</sup>); our results agree within  $0.5\%$  for both phases, see Table I. Additionally, from  $E$  vs.  $V$  (Fig. 7), we use eq. A1 in<sup>63</sup> to estimate the linear thermal expansion. In the stable FM phase we get  $\alpha_L = 6.5 \times 10^{-6} \text{ K}^{-1}$ , in agreement with the measured values of  $6.7 \pm 0.3 \times 10^{-6} \text{ K}^{-12}$  and  $6 \times 10^{-6} \text{ K}^{-18}$ .

However, for the AFM B2 structure the calculated<sup>63</sup>

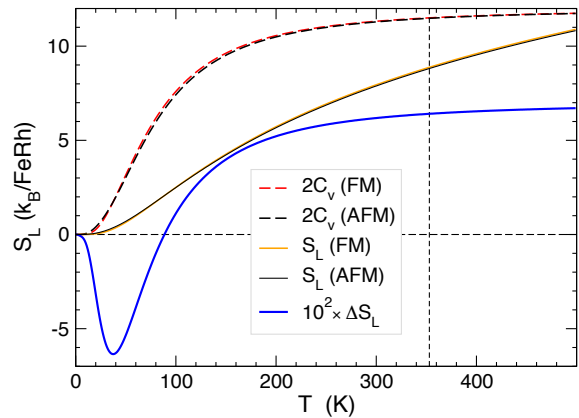


FIG. 6. (Color online). Heat capacity  $C_V$ , lattice entropy  $S_L$ , and  $\Delta S_L(\text{FM-AFM})$  for B2 structures from the phonon DOS in Fig. 3, calculated using  $d(T_c) \approx 0.06 \text{ \AA}$  from Fig. 4. The vertical dashed line is at  $T_c = 353 \text{ K}$ .

( $6.5 \times 10^{-6} \text{ K}^{-1}$ ) and experimental<sup>2</sup> ( $9.5 \times 10^{-6} \text{ K}^{-1}$ ) values differ by  $46\%$ . This disagreement indicates that the experimental structure is not precisely B2. Indeed, AFM B2 structure is unstable, while the suggested stable AFM structure is orthorhombic (see<sup>56</sup>), and its calculated linear thermal expansion coefficients along  $a$ ,  $b$ , and  $c$  axes are  $14$ ,  $16$ , and  $21 \times 10^{-6} \text{ K}^{-1}$ , respectively. Thus, the averaged uniform linear thermal expansion for the martensite (orthorhombic phase) is  $17 \times 10^{-6} \text{ K}^{-1}$ .

The austenitic cubic B2 phase has a premartensitic instability. Its structure at room  $T$  is neither ideal B2 nor the stable orthorhombic. As expected, its measured linear thermal expansion coefficient of  $9.5 \times 10^{-6} \text{ K}^{-1}$  is between the calculated values of  $6.5 \times 10^{-6} \text{ K}^{-1}$  for the unstable ideal B2 and  $17 \times 10^{-6} \text{ K}^{-1}$  for the martensite.

Notably, the estimate (formulated in<sup>63</sup>) ignores in-

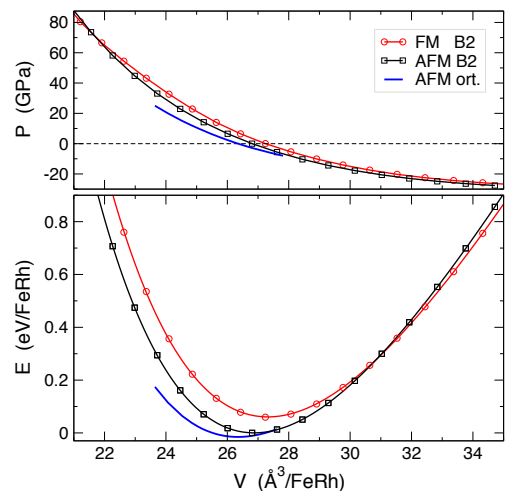


FIG. 7. (Color online). Pressure  $P$  (GPa) and energy  $E$  (eV) vs. volume  $V$  ( $\text{\AA}^3$ ) per FeRh formula unit for FM B2, AFM B2, and AFM orthorhombic structures.

ternal atomic motion. This approximation is acceptable for the stable FM phase, but not for the AFM B2 FeRh. To address the AFM B2 phase, taking into account atomic motion, we calculate phonon entropy at two lattice constants and use the relation  $(\partial S/\partial V)_P/K = \alpha_V$ , where the bulk modulus is  $K = -V(\partial P/\partial V) = V(\partial^2 E/\partial V^2)$  and the volumetric thermal expansion is  $\alpha_V \approx 3\alpha_L$ . From  $E(V)$  dependence in Fig. 7, we find  $K \approx 200$  GPa ( $1.25$  eV/Å<sup>3</sup>), while the lattice entropy at 353 K is  $7.68 k_B/\text{FeRh}$  at  $a = 2.887$  Å and  $8.82 k_B/\text{FeRh}$  at  $2.997$  Å, which gives  $(\partial S/\partial V) = 0.4 k_B/\text{Å}^3$ , so that  $\alpha_V = 2.75 \times 10^{-5} \text{ K}^{-1}$  and  $\alpha_L = 9.2 \times 10^{-6} \text{ K}^{-1}$ , which compares well with the measured  $9.5 \times 10^{-6} \text{ K}^{-12}$ . These results show how sensitive calculated responses are for systems with instabilities, as found in all caloric systems. The more careful estimates made here appear reliable for these systems.

### C. Magnetostructural transformation

The magnetostructural AFM-to-FM transformation is accompanied by a change of volume (Fig. 7) and electronic structure (Fig. 8). While electronic transformations happens with the speed of light  $c_{\text{light}}$ , a structural transformation (including volume change) propagates no faster than the speed of sound  $v_{\text{sound}} \ll c_{\text{light}}$ <sup>64</sup>. The electronic transformation is accompanied by discontinuity in pressure, which drives the volume change<sup>58</sup>. Possible causes for the electronic transformation include initial structure change or application of an external field. In particular, the magnetostructural transformation of FeRh can be caused by an application of an external magnetic field and/or stress, as well as thermal expansion.

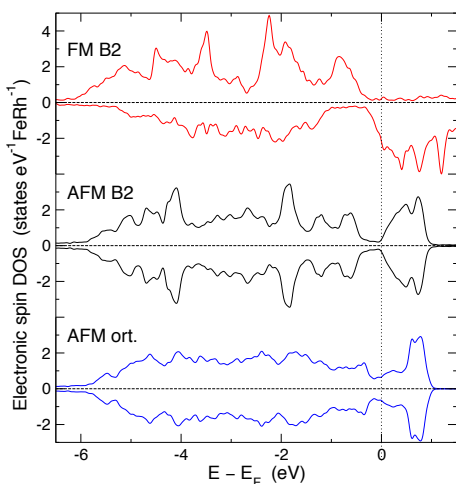


FIG. 8. (Color online). Electronic DOS of the ideal cubic B2 structure with FM (upper) and AFM (middle) spin ordering, and the AFM orthorhombic structure (lower) at  $P=0$ .

### D. Estimate of $T_c$

For fully relaxed structures at zero pressure, the calculated energy difference  $\delta E_0$  between unstable AFM and stable FM B2 is 29.8 meV/atom (Fig. 7) and compares well with previous calculations<sup>30</sup>. The transition temperature estimate is  $T_c = \delta E_0/k_B$  (eq. 3.7 in<sup>65</sup>), yielding 346 K, which compares well with 353 K from experiments on Fe<sub>50</sub>Rh<sub>50</sub><sup>15</sup>. This predicted value could have been used independent of experiment to evaluate the phonon contributions. Notably, this simple estimate (eq. 3.7 in<sup>65</sup>) is applicable to both stoichiometric (50 at.% Rh) and off-stoichiometric FeRh with partial atomic disorder.

From the electronic density of states (DOS,  $n(E)$ ) in Fig. 8, which agrees with all recent calculations<sup>38-40</sup>, we expect that lowering of the Fermi energy  $E_F$  (e.g., due to decrease in %Rh) will stabilize the FM phase, with a lesser effect on the AFM phase. This change will decrease the energy difference between the FM and AFM phases, and must reduce  $T_c$ . Indeed, this theoretical expectation agrees with the experimental phase diagram<sup>15,21,59</sup>.

### E. Estimate of $dT_c/dB$

The calculated magnetization of the fully relaxed AFM and FM FeRh B2 structures is 0 and  $2.1 \mu_B/\text{atom}$ , respectively. Using the upper bound for the magnetization change  $\Delta M(T_c) < [M(\text{FM}) - M(\text{AFM})]$  during the metamagnetic transformation, we find  $-dT_c/dB = \Delta M/\Delta S_T < 2.1 \mu_B/0.103 k_B = 13.7$  K/Tesla. However, a more realistic value<sup>26</sup> is that of  $\Delta M(T_c)$  at 60% of this upper bound, and gives  $-dT_c/dB = 8.2$  K/Tesla for the stoichiometric FeRh. Measurements of  $T_c(B)$  in the external magnetic field (or critical field vs.  $T$ ) provide a quadratic<sup>18</sup> dependence with the linear<sup>16</sup> slope  $-dT_c/dB$  in small fields of 8.2 in FeRh<sup>1</sup>; 8.2 in Fe<sub>49.5</sub>Rh<sub>50.5</sub><sup>26</sup>; 8.5 in Fe<sub>49</sub>Rh<sub>51</sub><sup>5</sup>; and from 9.6 to 9.7 K/Tesla<sup>46</sup> in Fe<sub>49</sub>Rh<sub>51</sub>.

### F. Electronic Entropy

In the AFM structure, the spin density around Rh sums to zero due to symmetry. Comparing the total electronic DOS at the Fermi energy,  $n(E_F)$ , in the FM and AFM states (Fig. 8), one can see that it changes substantially during the phase transformation from 2.310 (FM) to 0.677 (AFM) states eV<sup>-1</sup> per FeRh. This indicates that one should anticipate a large contribution of electronic entropy to the total entropy change  $\Delta S_T(T_c)$ .

Via Sommerfeld's expansion, the electronic entropy estimate is  $S_e \approx (\pi^2/3) \cdot k_B^2 T \cdot n(E_F)$ , i.e., 0.23 (FM) and 0.07 (AFM)  $k_B/\text{FeRh}$ . The difference  $\Delta S_e$  of 0.163  $k_B/\text{FeRh}$  (or 0.08  $k_B$  per atom) is the leading contribution to the total  $\Delta S_T$ , in agreement with prediction of Ponomarev<sup>6</sup> and its recent confirmation<sup>34</sup>.

## G. Entropy change

The total entropy has the lattice (L), electronic (e), and magnetic (m) contributions:  $S = S_L + S_e + S_m$ . We calculate entropy change  $\Delta S = S(FM) - S(AFM)$  due to electronic transformation at  $T_c = 353$  K at fixed lattice constant  $a = 2.997$  Å (measured<sup>2</sup> in the Fe<sub>50</sub>Rh<sub>50</sub> FM phase at  $T_c$ ). Neglecting the magnetic entropy change, which is a difference of rather small values of  $S_m$  in the fully ordered FM and AFM phases, we get the total entropy change  $\Delta S_T = 0.227 k_B/\text{FeRh}$ , or  $0.11 k_B/\text{atom}$  (i.e.,  $11.9 \text{ J kg}^{-1} \text{ K}^{-1}$ ), for the metamagnetic transformation at  $T_c$  at fixed volume. The experimentally assessed values of  $\Delta S_T$  range from 12 to  $14 \text{ J kg}^{-1} \text{ K}^{-1}$ ,<sup>5,46</sup> depending on the method<sup>5</sup>, sample composition<sup>1</sup>, and preparation<sup>3</sup>, see Table I. An early theoretical estimate<sup>6</sup> was  $\Delta S_T = 18.3 \text{ J kg}^{-1} \text{ K}^{-1}$  and  $\Delta T_S = -T_c \Delta S_T / C_B = -(20 \pm 2) \text{ K}$  for the temperature change at constant entropy. Here  $C_B(B, T)$  is the heat capacity at constant magnetic field  $B$ .

## H. Caloric effect

Using the asymptotic limit  $C_B \approx 3k_B/\text{atom}$  (or  $314 \text{ J} \cdot \text{kg}^{-1} \text{ K}^{-1}$ ) for solid FeRh at  $T \geq 300$  K (Fig. 6), the maximal isentropic temperature change is  $\Delta T_S = -T_c \Delta S_T / C_B = -13$  K. This estimate agrees with assessments<sup>5</sup>, ranging from  $-10.6$  to  $-12$  K, see Table I. The directly measured adiabatic temperature change  $\Delta T_{ad}(\Delta B)$ , produced by an added external field of  $\Delta B = 1.95$  Tesla, is as large as  $-12.9$  K for the quenched Fe<sub>49</sub>Rh<sub>51</sub> samples<sup>3</sup>.

## III. SUMMARY

For the FeRh, which exhibits a large caloric response arising from electronic and lattice contributions, we presented approximate methods (“fast estimators”) and evaluated a number of properties, including phonons, specific heat, lattice entropy, bulk modulus, thermal expansion coefficients, transition temperature, and caloric

effect. Our predicted properties are in quantitative agreement with experiment, see Table I. Our results verify that these fast estimators are reliable if applied carefully, and that the caloric behavior can be predicted accurately.

We confirmed that the AFM(111) B2 FeRh structure is unstable to distortions corresponding to M-point phonons. We presented a faster but approximate method to calculate phonons and evaluate lattice entropy  $S_L$  more reliably, taking into account the sensitive of phonon modes to the amplitude of atomic displacements for anharmonic or unstable modes (found for FM and AFM B2 FeRh). In particular, at the metamagnetic  $T_c$ , we applied the quasiharmonic approximation to single-atom displacements  $d$  with a “thermal” potential energy  $E(d) = \frac{1}{2} k_B T$ , separately evaluated in each system and for each atomic displacement (Fig. 4). The simple, but reliable, estimate for the metamagnetic transition temperature gives 346 K and compares well to the observed 353 K<sup>15</sup>. We applied a simplified estimate for thermal expansion, accurate when no internal cell relaxations occur, and then extended it by using phonon entropy from two lattice constants in more complex cases. These methods pave the way for theoretically guided searches (enhanced by machine-learning) for new caloric materials, when combined with key caloric correlation quantities (ongoing work).

## ACKNOWLEDGMENTS

Applications to caloric materials discovery at Ames Laboratory is supported by the U.S. Department of Energy (DOE), Advanced Manufacturing Office of the Office of Energy Efficiency and Renewable Energy through CaloriCool<sup>TM</sup> – the Caloric Materials Consortium established as a part of the U.S. DOE Energy Materials Network. In part, predictive methods development was funded by the U.S. DOE, Office of Science, Basic Energy Sciences, Materials Science and Engineering Division. Ames Laboratory is operated for the U.S. DOE by Iowa State University under contract DE-AC02-07CH11358.

## Appendix A: Computational Details

DFT calculations were performed using the modified<sup>66</sup> VASP code<sup>67,68</sup>. We used the projector augmented waves (PAW)<sup>69,70</sup> and PBE exchange-correlation functional<sup>71</sup> with Vosko-Wilk-Nusair spin-polarisation<sup>72</sup>. We used the modified Broyden method<sup>73</sup> for accelerating convergence. The Brillouin zone integration was performed on a dense Monkhorst-Pack mesh<sup>74</sup> with  $\geq 50$   $k$ -points per Å<sup>-1</sup>, including  $\Gamma$ . The cut-off energy for the plane wave basis set was increased to 334.9 eV (and 511.4 eV for the augmentation charge) by the high-precision flag. Phonons were calculated using the Phon code<sup>61</sup>. The atomic displacements varied from 0.04 to 0.12 Å in a cubic  $4 \times 4 \times 4$  supercell containing 64 FeRh formula units (128 atoms).

	Theory	Expt.	Units	Ref.
$M$ (FM)	149	$\approx 150$	$\text{A m}^2 \text{ kg}^{-1}$	<sup>26</sup>
$a$ (FM)	3.012	2.997	Å	<sup>2,16</sup>
$a$ (AF)	2.996	2.987	Å	<sup>2,16</sup>
$\alpha_L$ (FM B2)	6.5	6–6.7	$\times 10^{-6} \text{ K}^{-1}$	<sup>2,8</sup>
$\alpha_L$ (AF B2)	9.2	9.5	$\times 10^{-6} \text{ K}^{-1}$	<sup>2</sup>
$\alpha_L$ (AF ort)	17	-	$\times 10^{-6} \text{ K}^{-1}$	
$\Delta S_T(T_c)$	11.9	12–14	$\text{J kg}^{-1} \text{ K}^{-1}$	<sup>5,46</sup>
$-\Delta T_S$	13	11–13	K	<sup>5,46</sup>
$T_c$ (AF-FM)	346	353	K	<sup>15</sup>

TABLE I. Present predictions compared to experiment.

- \* zarkev@ameslab.gov  
† ddj@iastate.edu, ddj@ameslab.gov
- <sup>1</sup> J.S. Kouvel, *J. Appl. Phys.* **37**, 1257 (1966).
  - <sup>2</sup> L. Zsoldos, *Physica Status Solidi (B)* **20**, K25 (1967).
  - <sup>3</sup> S. Nikitin, G. Myalikgulyev, A. Tishin, M. Annaorazov, K. Asatryan, and A. Tyurin, *Physics Letters A* **148**, 363 (1990).
  - <sup>4</sup> M. P. Annaorazov, S. A. Nikitin, A. L. Tyurin, K. A. Asatryan, and A. K. Dovletov, *J. Appl. Phys.* **79**, 1689 (1996).
  - <sup>5</sup> A. Chirkova, K. Skokov, L. Schultz, N. Baranov, O. Gutfleisch, and T. Woodcock, *Acta Materialia* **106**, 15 (2016).
  - <sup>6</sup> B.K. Ponomarev, *Soviet Physics JETP* **36**, 105 (1973), translated from *Zh. Eksp. Teor. Fiz.* 63, 199–204 (1972).
  - <sup>7</sup> M. Pugacheva, J. Morkowski, A. Jezierski, and A. Szajek, *Solid State Communications* **92**, 731 (1994).
  - <sup>8</sup> M. R. Ibarra and P. A. Algarabel, *Phys. Rev. B* **50**, 4196 (1994).
  - <sup>9</sup> N. A. Zarkevich and D. D. Johnson, *Phys. Rev. Lett.* **113**, 265701 (2014).
  - <sup>10</sup> N. A. Zarkevich and D. D. Johnson, *Phys. Rev. B* **90**, 060102 (2014).
  - <sup>11</sup> M. Fallot, *Ann. Phys. (Paris)* **10**, 291 (1938).
  - <sup>12</sup> M. Fallot, *Rev. Sci.* **77**, 498 (1939).
  - <sup>13</sup> F. de Bergevin and L. Muldawaer, *Compt. Rend.* **252**, 1347 (1961).
  - <sup>14</sup> J. S. Kouvel and C. C. Hartelius, *J. Appl. Phys.* **33**, 1343 (1962).
  - <sup>15</sup> G. Shirane, C. W. Chen, P. A. Flinn, and R. Nathans, *Phys. Rev.* **131**, 183 (1963).
  - <sup>16</sup> A. Zakharov, A. Kadomtseva, R. Levitin, and E. Ponyatovskii, *Soviet Physics JETP* **19**, 1348 (1964), translated from: *Zh. Eksp. Teor. Fiz.* **46** (6), 2003–2010 (1964).
  - <sup>17</sup> G. Shirane, R. Nathans, and C. W. Chen, *Phys. Rev.* **134**, A1547 (1964).
  - <sup>18</sup> J. B. McKinnon, D. Melville, and E. W. Lee, *J. Phys. C: Solid State Physics* **3**, S46 (1970).
  - <sup>19</sup> L. Vinokurova, A. Vlasov, N. Kulikov, and M. Pardavi-Horváth, *J. Magn. Magn. Mater.* **25**, 201 (1981).
  - <sup>20</sup> M. Annaorazov, K. Asatryan, G. Myalikgulyev, S. Nikitin, A. Tishin, and A. Tyurin, *Cryogenics* **32**, 867 (1992).
  - <sup>21</sup> J. Balun, L. Eleno, and G. Inden, *Intermetallics* **15**, 1237 (2007).
  - <sup>22</sup> S. Inoue, H. Yu Yu Ko, and T. Suzuki, *IEEE Trans. Magnetics* **44**, 2875 (2008).
  - <sup>23</sup> I. Radu, C. Stamm, N. Pontius, T. Kachel, P. Ramm, J.-U. Thiele, H. A. Dürr, and C. H. Back, *Phys. Rev. B* **81**, 104415 (2010).
  - <sup>24</sup> D. W. Cooke, F. Hellman, C. Baldasseroni, C. Bordel, S. Moyerman, and E. E. Fullerton, *Phys. Rev. Lett.* **109**, 255901 (2012).
  - <sup>25</sup> Y. Wakisaka, Y. Uemura, T. Yokoyama, H. Asakura, H. Morimoto, M. Tabuchi, D. Ohshima, T. Kato, and S. Iwata, *Phys. Rev. B* **92**, 184408 (2015).
  - <sup>26</sup> R. Onodera, K. Ohtake, K. Takahashi, S. Kimura, K. Watanabe, and K. Koyama, *Journal of the Japan Institute of Metals and Materials* **80**, 186 (2016).
  - <sup>27</sup> F. Pressacco, V. Uhlř, M. Gatti, A. Bendounan, E. E. Fullerton, and F. Sirotti, *Scientific Reports* **6**, 22383 (2016).
  - <sup>28</sup> N.P. Grazhdankina, *Soviet Physics Uspekhi* **11**, 727 (1969).
  - <sup>29</sup> H. Hasegawa, *J. Magn. Magn. Mater.* **66**, 175 (1987).
  - <sup>30</sup> V. L. Moruzzi and P. M. Marcus, *Phys. Rev. B* **46**, 2864 (1992).
  - <sup>31</sup> V. L. Moruzzi and P. M. Marcus, *Phys. Rev. B* **46**, 14198 (1992).
  - <sup>32</sup> C. Paduani, *J. Appl. Phys.* **90**, 6251 (2001).
  - <sup>33</sup> L. M. Sandratskii and P. Mavropoulos, *Phys. Rev. B* **83**, 174408 (2011).
  - <sup>34</sup> J. B. Staunton, R. Banerjee, M. d. S. Dias, A. Deak, and L. Szunyogh, *Phys. Rev. B* **89**, 054427 (2014).
  - <sup>35</sup> J. Kudrnovský, V. Drchal, and I. Turek, *Phys. Rev. B* **91**, 014435 (2015).
  - <sup>36</sup> E. Mendive-Tapia and T. Castán, *Phys. Rev. B* **91**, 224421 (2015).
  - <sup>37</sup> J. Barker and R. W. Chantrell, *Phys. Rev. B* **92**, 094402 (2015).
  - <sup>38</sup> S. Polesya, S. Mankovsky, D. Ködderitzsch, J. Minár, and H. Ebert, *Phys. Rev. B* **93**, 024423 (2016).
  - <sup>39</sup> U. Aschauer, R. Braddell, S. A. Brechbühl, P. M. Derlet, and N. A. Spaldin, *Phys. Rev. B* **94**, 014109 (2016).
  - <sup>40</sup> M. Wolloch, M. E. Gruner, W. Keune, P. Mohn, J. Redinger, F. Hofer, D. Suess, R. Podloucky, J. Landers, S. Salamon, F. Scheibel, D. Spoddig, R. Witte, B. Roldan Cuenya, O. Gutfleisch, M. Y. Hu, J. Zhao, T. Toellner, E. E. Alp, M. Siewert, P. Entel, R. Pentcheva, and H. Wende, *Phys. Rev. B* **94**, 174435 (2016).
  - <sup>41</sup> J. Kim, R. Ramesh, and N. Kioussis, *Phys. Rev. B* **94**, 180407(R) (2016).
  - <sup>42</sup> U.S. Geological Survey, “Mineral industry surveys,” <https://minerals.usgs.gov/minerals/pubs/commodity/platinum/mis-201703-plati.pdf> (2017).
  - <sup>43</sup> U.S. Geological Survey, “2012 minerals yearbook: Platinum-group metals,” <https://minerals.usgs.gov/minerals/pubs/commodity/platinum/myb1-2012-plati.pdf> (2012).
  - <sup>44</sup> M. Manekar and S. B. Roy, *J. Phys. D: Applied Physics* **41**, 192004 (2008).
  - <sup>45</sup> K. G. Sandeman, *Scripta Materialia* **67**, 566 (2012).
  - <sup>46</sup> E. Stern-Taulats, A. Planes, P. Lloveras, M. Barrio, J.-L. Tamarit, S. Pramanick, S. Majumdar, C. Frontera, and L. Mañosa, *Phys. Rev. B* **89**, 214105 (2014).
  - <sup>47</sup> Y. Liu, L. C. Phillips, R. Mattana, M. Bibes, A. Barthélémy, and B. Dkhil, *Nature Communications* **7**, 11614 (2016).
  - <sup>48</sup> J.-U. Thiele, S. Maat, and E. E. Fullerton, *Appl. Phys. Lett.* **82**, 2859 (2003).
  - <sup>49</sup> G. Ju, J. Hohlfeld, B. Bergman, R. J. M. van de Veerdonk, O. N. Mryasov, J.-Y. Kim, X. Wu, D. Weller, and B. Koopmans, *Phys. Rev. Lett.* **93**, 197403 (2004).
  - <sup>50</sup> J. U. Thiele, S. Maat, J. L. Robertson, and E. E. Fullerton, *IEEE Transactions on Magnetics* **40**, 2537 (2004).
  - <sup>51</sup> R. Fan, C. J. Kinane, T. R. Charlton, R. Dorner, M. Ali, M. A. de Vries, R. M. D. Brydson, C. H. Marrows, B. J. Hickey, D. A. Arena, B. K. Tanner, G. Nisbet, and S. Langridge, *Phys. Rev. B* **82**, 184418 (2010).
  - <sup>52</sup> R. O. Cherifi, V. Ivanovskaya, L. C. Phillips, A. Zobelli, I. C. Infante, E. Jacquet, V. Garcia, S. Fusil, P. R. Briddon, N. Guiblin, A. Mougín, A. A. Únal, F. Kronast, S. Valencia, B. Dkhil, A. Barthélémy, and M. Bibes, *Nat. Mater.*

- 13**, 345 (2014).
- <sup>53</sup> X. Marti, I. Fina, C. Frontera, J. Liu, P. Wadley, Q. He, R. J. Paull, J. D. Clarkson, J. Kudrnovsky, I. Turek, J. Kunes, D. Yi, J.-H. Chu, C. T. Nelson, L. You, E. Arenholz, S. Salahuddin, J. Fontcuberta, T. Jungwirth, and R. Ramesh, *Nat. Mater.* **13**, 367 (2014).
- <sup>54</sup> Z. Q. Liu, L. Li, Z. Gai, J. D. Clarkson, S. L. Hsu, A. T. Wong, L. S. Fan, M.-W. Lin, C. M. Rouleau, T. Z. Ward, H. N. Lee, A. S. Sefat, H. M. Christen, and R. Ramesh, *Phys. Rev. Lett.* **116**, 097203 (2016).
- <sup>55</sup> X. Zhou, F. Matthes, D. E. Bürgler, and C. M. Schneider, *AIP Advances* **6**, 015211 (2016).
- <sup>56</sup> N. A. Zarkevich and D. D. Johnson, *Phys. Rev. B* **submitted** (2017).
- <sup>57</sup> D. Sheppard, P. H. Xiao, W. Chemelewski, D. D. Johnson, and G. Henkelman, *J. Chem. Phys.* **136**, 074103 (2012).
- <sup>58</sup> N. A. Zarkevich and D. D. Johnson, *J. Chem. Phys.* **143**, 064707 (2015).
- <sup>59</sup> L. Swartzendruber, *Bulletin of Alloy Phase Diagrams* **5**, 456 (1984).
- <sup>60</sup> N. A. Zarkevich, *Complexity* **11**, 36 (2006).
- <sup>61</sup> D. Alfè, *Computer Physics Communications* **180**, 2622 (2009).
- <sup>62</sup> N.A. Zarkevich, “Thermophonon code,” [http://lib.dr.iastate.edu/ameslab\\_software/2/](http://lib.dr.iastate.edu/ameslab_software/2/) (2014).
- <sup>63</sup> N. A. Zarkevich, E. H. Majzoub, and D. D. Johnson, *Phys. Rev. B* **89**, 134308 (2014).
- <sup>64</sup> N. A. Zarkevich and D. D. Johnson, *Physical Review B* **91**, 174104 (2015).
- <sup>65</sup> N. A. Zarkevich, *First-principles prediction of thermodynamics and ordering in metallic alloys*, Ph.D. thesis, University of Illinois at Urbana-Champaign (2003).
- <sup>66</sup> N. A. Zarkevich and D. D. Johnson, *J. Chem. Phys.* **142**, 024106 (2015).
- <sup>67</sup> G. Kresse and J. Hafner, *Phys. Rev. B* **47**, RC558 (1993).
- <sup>68</sup> G. Kresse, and J. Hafner, *Phys. Rev. B* **49**, 14251 (1994).
- <sup>69</sup> P. E. Blöchl, *Phys. Rev. B* **50**, 17953 (1994).
- <sup>70</sup> G. Kresse, and D. Joubert, *Phys. Rev. B* **59**, 1758 (1999).
- <sup>71</sup> J. P. Perdew, K. Burke, and M. Ernzerhof, *Phys. Rev. Lett.* **77**, 3865 (1996).
- <sup>72</sup> S. H. Vosko, L. Wilk, and M. Nusair, *Can. J. Phys.* **58**, 1200 (1980).
- <sup>73</sup> D. D. Johnson, *Phys. Rev. B* **38**, 12807 (1988).
- <sup>74</sup> H. J. Monkhorst and J. D. Pack, *Phys. Rev. B* **13**, 5188 (1976).